LETTERS
https://doi.org/10.1038/s41558-019-0546-1

nature climate change

Antarctic iceberg impacts on future Southern Hemisphere climate

Fabian Schloesser[1,2], Tobias Friedrich[1,2], Axel Timmermann[3,4*], Robert M. DeConto[5] and David Pollard[6]

Future iceberg and meltwater discharge from the Antarctic ice sheet (AIS) could substantially exceed present levels, with strong implications for future climate and sea levels. Recent climate model simulations on the impact of a rapid disintegration of the AIS on climate have applied idealized freshwater forcing scenarios[1,2] rather than the more realistic iceberg forcing. Here we use a coupled climate–iceberg model to determine the climatic effects of combined iceberg latent heat of fusion and freshwater forcing. The iceberg forcing is derived from an ensemble of future simulations conducted using the Penn State ice-sheet model[3]. In agreement with previous studies, the simulated AIS meltwater forcing causes a substantial delay in greenhouse warming in the Southern Hemisphere and activates a transient positive feedback between surface freshening, subsurface warming and ice-sheet/shelf melting, which can last for about 100 years and may contribute to an accelerated ice loss around Antarctica. However, accounting further for the oceanic heat loss due to iceberg melting considerably increases the surface cooling effect and reduces the subsurface temperature feedback amplitude. Our findings document the importance of considering realistic climate–ice sheet–iceberg coupling for future climate and sea-level projections.

Recent ice-sheet simulations suggest that future AIS discharge could increase substantially towards the end of this century, attaining values of >1 Sv ($1\,\mathrm{Sv} = 10^6\,\mathrm{m^3\,s^{-1}} \approx 31{,}500\,\mathrm{Gt\,yr^{-1}} \approx 0.087$ m sea-level equivalent (SLE) $\mathrm{yr^{-1}}$)[3–6]. With AIS discharge causing reduced Southern Hemisphere surface temperatures[1,7–12], freshwater forcing of this magnitude could delay Southern Hemisphere greenhouse warming by up to several decades[2]. Moreover, AIS discharge has been shown to lead to increased subsurface ocean temperatures around Antarctica, which may provide a positive feedback to AIS melting[1,2,4,6,12–14].

Previous simulations have applied either climate forcing to ice-sheet models[3] or ice-sheet freshwater forcing to climate models[2]. Important feedbacks among atmosphere, ocean and the AIS are therefore not properly resolved. Moreover, the amplitude of future AIS discharge remains highly uncertain, even in response to specific warming scenarios[15]. Processes such as hydrofracturing, ice-cliff instability and basal melting are observationally not well constrained[5]. Resulting uncertainties translate into uncertainties in global sea-level projections and AIS discharge, which are reflected in substantial discrepancies between different state-of-the-art estimates of future contributions to sea-level changes from the AIS[2,3,5,6,15]. Models also do not agree well on the partition between basal melting and calving fluxes[6,16]. In more realistic scenarios, calving icebergs are advected by ocean currents and winds, influencing the ocean, sea ice and climate along their trajectories by continuously changing freshwater and heat fluxes[17,18]. Iceberg melting is also modulated seasonally, as sea ice, winds, ocean currents and temperatures change dramatically around Antarctica[19]. This fundamental process has not been properly included in future climate and sea-level projections.

To improve our understanding of the climatic response to future changes in the AIS, we use the earth system model of intermediate complexity (LOVECLIM, see Methods) under the representative concentration pathway (RCP) 4.5 and 8.5 GHG emission scenarios (RCP4.5 and RCP8.5, respectively). We further apply a wide range of freshwater and iceberg forcing scenarios derived from ice-sheet model simulations conducted with the Penn State ice-sheet model[16]. The low computational cost of LOVECLIM allows us to conduct a large number of ensemble simulations with varying AIS meltwater/iceberg discharge amplitude (Fig. 1; Methods). The thermodynamic and dynamic impacts of icebergs are tested by varying the implementation of AIS forcing in different experiments using the same AIS forcing scenario (Supplementary Table 1). Here, the thermodynamic effect of icebergs describes the consequences of energy consumption by the melting processes to account for latent heat. Icebergs can travel large distances before melting entirely, thereby generating spatiotemporally varying meltwater patterns that extend across the Southern Ocean[19,20]. This process is, henceforth, referred to as the dynamic iceberg effect. To isolate its climatic impact, simulations are compared to idealized experiments with spatially homogeneous freshwater forcing.

The oceanic response to Antarctic meltwater discharge is well documented in climate models[1,2,7–12]. By freshening the Southern Ocean surface water and lowering its density, AIS meltwater strengthens Southern Ocean stratification[1,7–12]. The latter acts as a barrier for deep convection, Antarctic bottom water formation and vertical heat fluxes, enhancing Southern Hemisphere sea-ice production and causing surface cooling and subsurface ocean warming around Antarctica[1,12,21]. The impact on global ocean circulation[22–24] then results in an interhemispheric asymmetry in surface temperature[25], a northward displacement of the intertropical convergence zone and global precipitation changes[22,26,27].

The response of LOVECLIM to freshwater forcing[1,6,7] is very similar to that recently reported using more sophisticated coupled general circulation models[2,22]. In control experiments with greenhouse forcing, but without AIS forcing, global surface air

[1]International Pacific Research Center, University of Hawaii at Manoa, Honolulu, HI, USA. [2]Department of Oceanography, University of Hawaii at Manoa, Honolulu, HI, USA. [3]Center for Climate Physics, Institute for Basic Science, Busan, Republic of Korea. [4]Pusan National University, Busan, Republic of Korea. [5]Department of Geosciences, University of Massachusetts, Amherst, MA, USA. [6]Earth and Environmental Systems Institute, Pennsylvania State University, University Park, PA, USA. *e-mail: timmermann@pusan.ac.kr

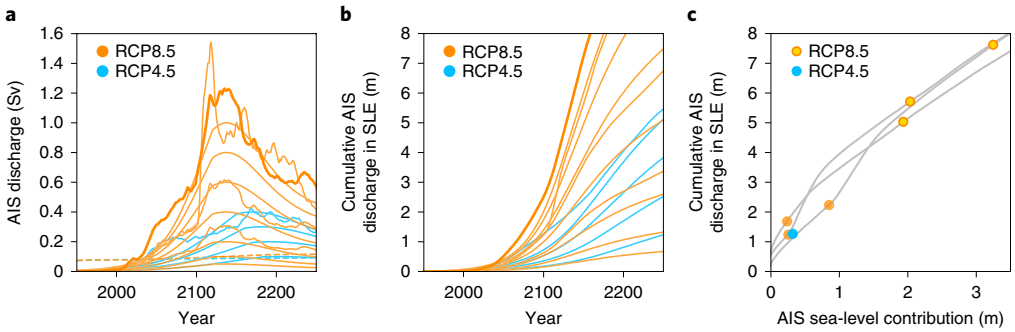

Fig. 1 | Meltwater forcing scenarios and associated AIS sea-level contribution. a, Simulated[3] and synthetic AIS discharge scenarios used—scenario AIS8.5 is indicated by the thicker orange line. Dashed curves indicate additional liquid runoff balancing precipitation over Antarctica (Methods). **b**, Cumulative AIS discharge in SLE. **c**, Cumulative AIS discharge in SLE as a function of AIS global mean sea-level contribution for simulated scenarios[3]. Dark (light) orange dots indicate that relationship for the RCP8.5 scenarios in 2100 (2150), and the blue dot the RCP4.5 scenario in 2100.

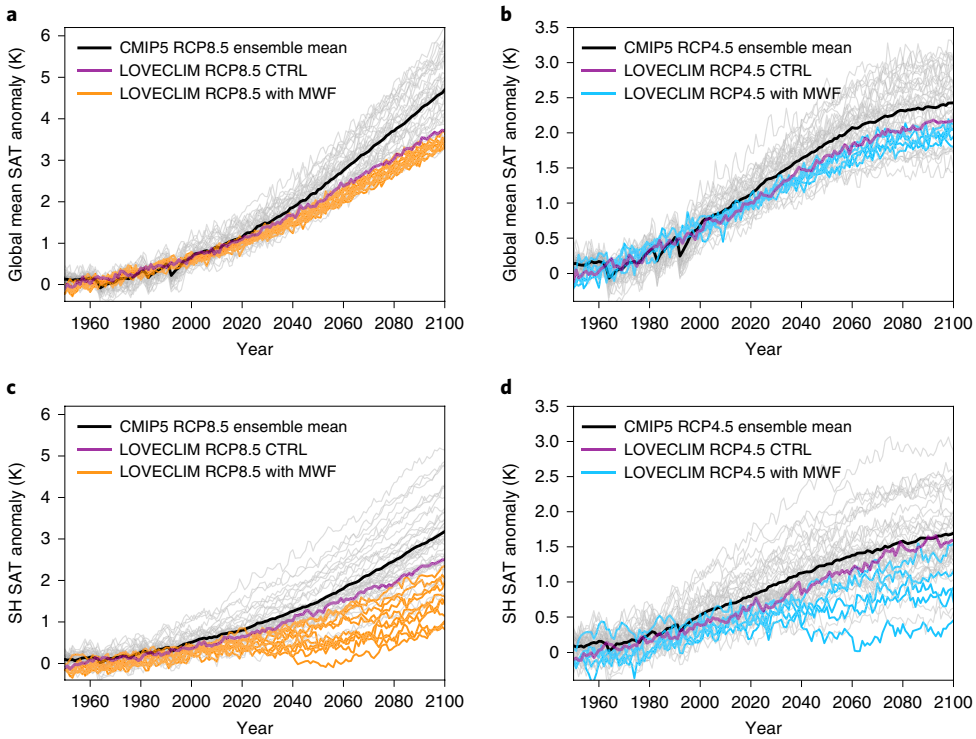

Fig. 2 | Uncertainty of global and Southern Hemisphere temperature trajectories related to AIS meltwater discharge. a–d, SAT anomaly (relative to 1900–1950 mean) averaged globally (**a**,**b**) and averaged in the Southern Hemisphere (SH) between 65 °S and 35 °S (**c**,**d**) for CMIP5 RCP8.5 (**a**,**c**) and RCP4.5 (**b**,**d**) ensemble means (black lines) and individual members (thin grey lines). SAT for LOVECLIM greenhouse warming control (CTRL) experiments without MWF (RCP8.5–CTR and RCP4.5–CTR), the same variables are indicated by purple lines; orange and blue lines correspond to LOVECLIM greenhouse warming experiments with MWF for scenarios RCP8.5 and RCP4.5, respectively, using the standard set-up (see Methods).

temperature (SAT) increased by about 4 and 2 K from 1950 to 2100 in response to RCP8.5 and RCP4.5 GHG forcing (Fig. 2a,b), respectively, which is at the lower end of the range of the Coupled Model Intercomparison Project Phase 5 (CIMP5) model response. The strongest meltwater forcing (MWF) considered in the present study (Fig. 1a, thicker orange curve, corresponding to an RCP8.5 ice-sheet response scenario[3], which is substantially stronger than other estimates[5,15]) reduces global averaged warming in the year 2100 by about 0.5 K (Fig. 2a,b), which is not insignificant but relatively modest on the global scale compared to the overall CMIP5 model spread.

In contrast, Southern Hemisphere (65 °S–35 °S) surface cooling (relative to greenhouse warming control simulations without AIS discharge) is strongly controlled by the AIS discharge amplitude (Fig. 3a,b). The cooling sensitivity—that is, the temperature difference per unit MWF—is strongest when the forcing is weak, such that even a relatively modest forcing of about 0.2 Sv could cool global SAT by 0.3 K (Fig. 3a). The cooling effect weakens with increased forcing amplitude, in particular for the RCP8.5 scenario, such that relative cooling is unlikely to exceed 0.6 K globally even with a rapidly retreating AIS.

Surface cooling is most pronounced in the Southern Hemisphere (Fig. 2c,d and 3b–f) and in regions covered by sea ice. It is strongest in regions where iceberg melting is concentrated, particularly in the 'iceberg alleys' in the Scotia Sea and northern Ross Sea, where

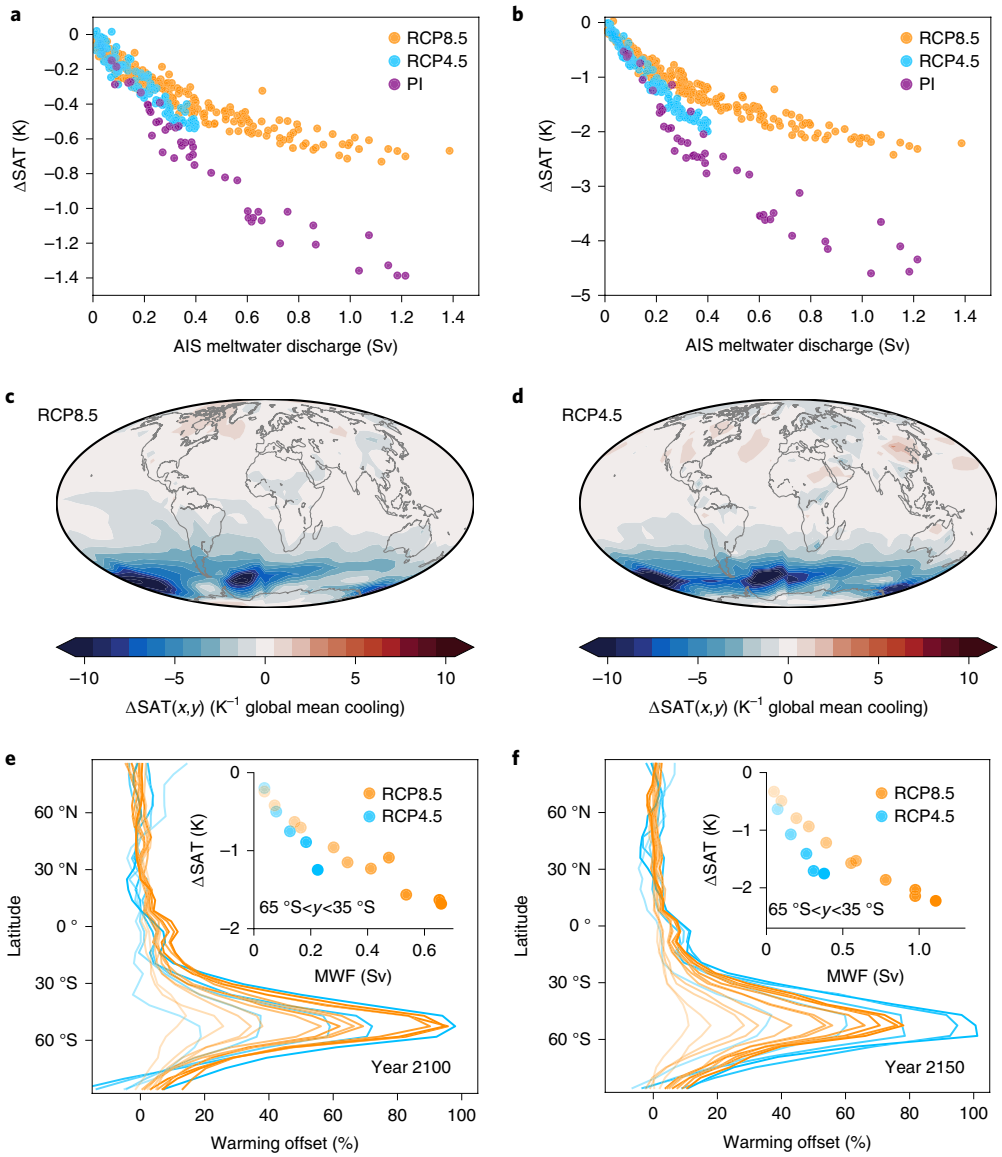

Fig. 3 | Impact of MWF on SAT. a, Decadal averages of global mean SAT difference between control (no AIS discharge) and experiments with AIS discharge, as a function of MWF strength between the years 2000 and 2250. Colours indicate GHG scenarios. **b**, As for SAT, averaged between 65 °S and 35 °S. **c**,**d**, Ensemble average of SAT difference (function of longitude *x* and latitude *y*) between the years 2090 and 2110 divided by global mean difference and weighted by strength of MWF for RCP8.5 (**c**) and RCP4.5 (**d**). **e**,**f**, Zonally averaged greenhouse warming offset caused by MWF for 20-year averages around the years 2100 (**e**) and 2150 (**f**). PI, pre-industrial.

icebergs first encounter warmer waters (Fig. 3c,d). In these regions, surface cooling reaches 6 K in the most extreme scenarios (Figs. 3c,d and 4a). Averaged over mid-range and high southern latitudes (65 °S–35 °S), strong MWF reduces temperatures by >1 °C and temporarily reverses the warming trend in some ensemble members over decades during the middle of the century (Fig. 2c,d). At these latitudes, the spread in temperature trajectories related to AIS discharge is comparable to that between different CMIP5 models without AIS forcing. Zonally averaged, cooling could offset a substantial portion of greenhouse warming in the Southern Hemisphere over the next century (Fig. 3e,f). On the other hand, the AIS effect on Northern Hemisphere temperatures is weak, implying that there would be no substantial delay in greenhouse warming in the Northern Hemisphere.

One process that contributes significantly to Southern Hemisphere cooling in the AIS discharge experiments is consumption of energy by melting segments of the AIS and icebergs[17]: sustaining a MWF of 1 Sv requires about 0.33 PW (1 PW = 10^{15} Watts) to account for latent heat (see Methods). With AIS discharge reaching peak values >1.5 Sv in RCP8.5 ice-sheet scenarios[3] (Fig. 1a), the melt heat required is of the same order as the average heat uptake of the global climate system over the past decade (0.3–0.5 PW)[28]. Since much of the AIS discharge is associated with oceanic melt, most of the energy is drawn from the Southern Ocean, amplifying the cooling in this region. Accordingly, SAT cooling is weaker in sensitivity experiments when melt heat is not accounted for in the model (Figs. 4b and 5). The relative importance of the melt heat effect is particularly pronounced in RCP8.5 scenarios, where elimination of melt heat reduces Southern Hemisphere cooling relative to the RCP8.5–CTR greenhouse warming simulation by about 75% (Figs. 4b and 5). This is due to a weakened cooling effect of freshwater forcing under transient RCP8.5 compared to pre-industrial conditions (Fig. 3a,b),

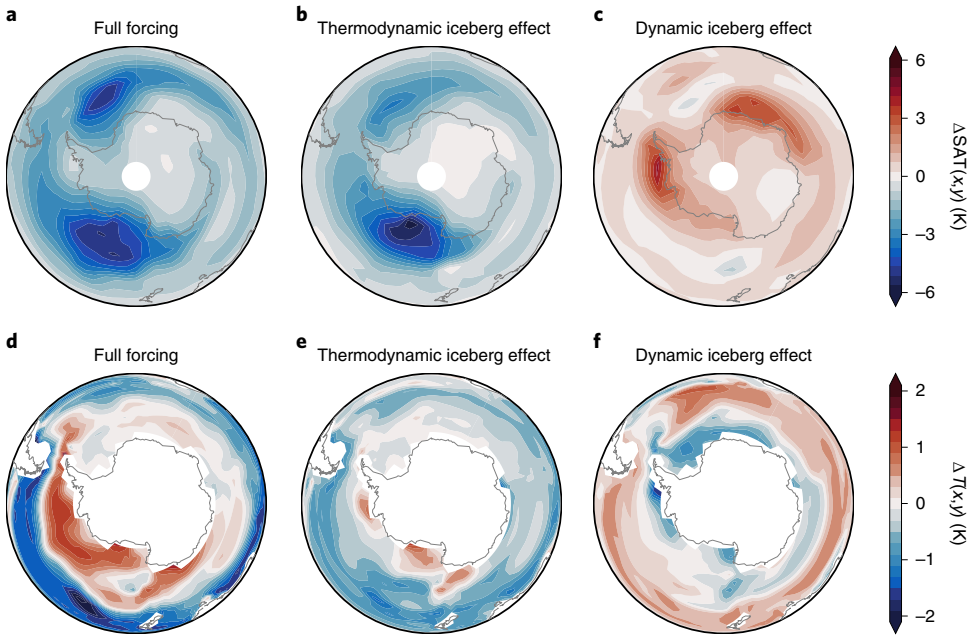

Fig. 4 | Impact of icebergs on SAT and subsurface ocean temperatures. a–c, SAT anomalies averaged over the years 2090–2110 with full iceberg model and forcing AIS8.5 relative to no forcing (Standard - RCP8.5-CTR, **a**), the thermodynamic effect—that is, full iceberg model minus iceberg model without latent heat (Standard - noLH, **b**) and the dynamic iceberg effect—that is, full iceberg model minus prescribed freshwater and heat fluxes (standard – mean of F70S and F50S, **c**). **d–f**, Corresponding ocean temperature (*T*) anomalies at 400 m depth.

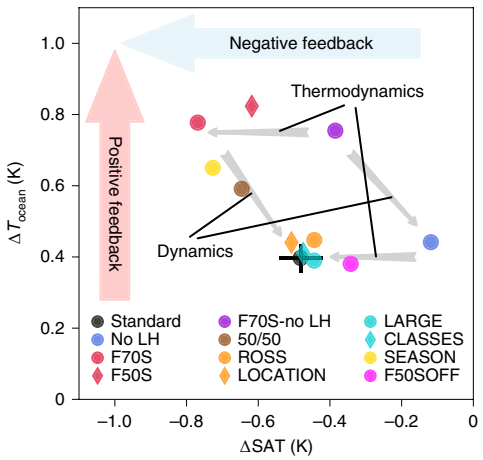

Fig. 5 | Impact of iceberg processes on ice–ocean feedback. Global surface air temperature anomalies versus 400-m ocean temperature anomalies south of 60 °S averaged over the years 2090–2110 for RCP8.5, with forcing AIS8.5 and different implementations of the iceberg model or surface freshwater and heat fluxes (see Methods). Anomalies are calculated relative to control experiments without AIS forcing. Black bars indicate two standard deviations from ensemble members for experiment Standard.

because ocean stratification is already being increased by surface warming and sea-ice production is reduced (Supplementary Fig. 3a). It is noteworthy that a similar effect applies to basal melting under ice shelves although LOVECLIM does not resolve the circulation in ice cavities, which could further modify the impact of meltwater[29].

The strength of the dynamic iceberg effect is dependent on a number of factors that are difficult to constrain with current climate and iceberg models[18]. In the simulated AIS scenarios, discharge is dominated by calving while the large ice shelves are disintegrating[16]; however, different models found other partitions between calving and basal melt[6]. Furthermore, while the present-day volumetric calving flux may be dominated by giant icebergs that melt predominantly off the Antarctic coast[19,20], future iceberg size distributions are unknown. For this reason, the iceberg model is implemented such that most iceberg melt occurs in iceberg alleys off the Antarctic coast—that is, the dynamic effects are relatively strong. The impact of this assumption is tested in a number of sensitivity experiments (see Methods).

Relative to two experiments with uniformly prescribed freshwater and heat fluxes over the area between the Antarctic coast and the latitude circles at 70 °S and 50 °S (F70S and F50S, respectively), both, surface cooling and subsurface ocean warming near Antarctica are reduced in the standard experiment (Figs. 4c,f and 5), which includes the dynamic and thermodynamic effects of icebergs. Compared to a similar experiment (F50SOFF), where the uniform MWF is applied to the area between 50 °S and two grid cells north of Antarctica such that no flux occurs along the Antarctic coast, the effect is opposite (Fig. 5). These results indicate that the impact of meltwater is most effective closest to Antarctica, where it leads to increased sea-ice production. The dramatic increase in subsurface warming without dynamic iceberg effect (by about 100%, Figs. 4f and 5) may be explained by MWF being particularly efficient in suppressing convection near the Antarctic coast and during winter, when iceberg melting is relatively weak. Consistently, the difference between iceberg and uniform flux experiments is reduced when a seasonal cycle is applied to the uniform flux (experiment SEASON, Fig. 5). When the MWF is partitioned equally between iceberg and uniform flux south of 70 °S (experiment 50/50, Fig. 5), surface cooling and subsurface warming is about half-way between the experiments where MWF is applied only one way or the other. This suggests that the spatially inhomogeneous freshwater and cooling effects of icebergs, referred to as dynamic effect, scale linearly with the ratio of ice volume being exported by icebergs away from the Antarctic coast.

Iceberg trajectories and melting respond to changes in ocean circulation and winds, such that they extend farther equatorward by 2100 than at the beginning of the twenty-first century (Supplementary Figs. 2 and 4). This is a consequence of the strengthened westerlies[1,30] (about 10% by 2100 in the RCP8.5 control), which accelerate the northward propagation of icebergs, as well as of the cooling of surface ocean temperatures, which in turn reduces melting rates (Fig. 4a). This iceberg response contributes to reduced cooling per unit forcing with increasing amplitude, particularly in the RCP8.5 experiments.

It has been proposed that MWF-driven subsurface ocean warming could provide a positive feedback by accelerating basal melting, leading to a positive feedback loop[1,2,4,6,12–14]. Using an iceberg model, the present results show a robust, almost linear relation between subsurface ocean temperature increase (averaged at 400-m depth, south of 60 °S) to about 0.3–0.4 K with 0.2 Sv freshwater and the iceberg thermodynamic effect over the twenty-first century (Supplementary Fig. 3b). Locally, the increase in subsurface ocean temperature could be higher: the maximum 10-year average of the 400-m ocean temperature anomalies south of 60 °S in 2100 increases from 0.5 K with no MWF (due to internal variability) to 1.5 K with 0.2 Sv. These findings support the positive feedback hypothesis.

On the other hand, strengthening of the AIS discharge beyond 0.3 Sv does not further increase subsurface temperatures (Supplementary Fig. 3b), thereby limiting positive feedback. In RCP8.5 scenario experiments, the subsurface ocean warming effect is reduced in the twenty-second century, with subsurface temperatures eventually being colder than in the control without AIS forcing in some experiments (Supplementary Fig. 3b). This indicates that surface cooling has a delayed effect on subsurface temperatures, with a timescale of a few decades, implying that a positive feedback loop cannot be effective on longer timescales, and that climate–ice-sheet feedbacks would instead lead to stabilization of melting rates. Perhaps even more importantly, cooling of Antarctic SAT in response to AIS discharge could slow down AIS melting and reduce rainfall and hydrofracturing, thereby providing a negative feedback (Fig. 5).

The relative impact of positive and negative feedbacks in ice models depends on processes including basal melting, hydrofracturing and ice-cliff instability that rely on more or less poorly constrained parameterizations[5]. The present results indicate that not only the amplitude of AIS discharge, but also the dynamic and thermodynamic iceberg effects (Fig. 5), can fundamentally impact the relative strengths of these feedbacks. Because of these issues, recent estimates of climate–ice-sheet coupling on future AIS melting[2,6], using simple scaling laws based on subsurface ocean warming or not considering the thermodynamic iceberg effect, remain highly uncertain.

Using the ESM2M model and the same AIS discharge scenario[3] as used here (Fig. 1a, thicker orange line), a recent study[2] reported weaker global SAT cooling (0.38 ± 0.02 K) but substantially stronger subsurface ocean temperature increases (~1.3 K ocean warming zonally averaged along the Antarctic coast at 400-m depth) than the corresponding effects simulated by LOVECLIM with iceberg model experiments reported here. Although these discrepancies could be due to model differences, it is noteworthy that they are also consistent with the different implementations of the AIS forcing as either freshwater[2] or combined freshwater and iceberg latent heat of fusion (Fig. 5). This suggests that the model response to AIS discharge forcing may be relatively robust, but illustrates that iceberg models are instrumental in simulating a realistic coupling between ocean and ice sheets.

These findings come with some caveats. Large-scale dynamic processes are implemented in LOVECLIM similarly as in other climate models suitable for century-scale simulations (for example, CMIP5), and the large-scale response to AIS forcing is qualitatively and quantitatively consistent with those reported in other studies. The coarse-resolution, three-degree ocean component, however, cannot resolve regional scale processes, such as the occasional intrusion of warm circumpolar deep water onto the continental shelf and circulation in ice cavities[29,31], and the local variability of the Antarctic coastal current. Through their effect on ocean temperatures over the Antarctic shelf, such processes can have significant impacts on basal melting and the pace of AIS disintegration. Hence, they are expected to play an important role in the coupling of climate and ice sheets. Furthermore, these processes impact sea-ice and deep-water formation and the export of ice and freshwater into the Southern Ocean. A resolution of about 1 km may be required to resolve Antarctic shelf processes[32], which is significantly finer than that of current global climate models for century-scale AIS ensemble simulations. An additional uncertainty is related to the iceberg size classes and trajectories, which substantially impact the export of ice off the Antarctic coast[18,19]. Our simulations indicate that the dynamic iceberg effect scales linearly with the ice export rate. More realistic simulations of ocean ice-sheet coupling require better constraints of ice-sheet model parameterizations; but iceberg size distributions associated with future ice-shelf retreat also need to be addressed.

Our findings show that, to project Southern Hemisphere future climate change and global sea-level rise, realistic climate–ice-sheet coupling needs to be taken into account. This includes not only the amplitude of freshwater fluxes released from the AIS, but also the thermodynamic and dynamic effects of melting icebergs on the ocean. Due to their impacts on both surface air and subsurface ocean temperatures, these effects could also critically impact the relative strength of positive and negative climate–ice-sheet feedback processes. The large uncertainty in future AIS melting translates to considerable uncertainties in future Southern Hemisphere climate change projections.

Online content

Any methods, additional references, Nature Research reporting summaries, source data, statements of code and data availability and associated accession codes are available at https://doi.org/10.1038/s41558-019-0546-1.

Received: 6 January 2019; Accepted: 19 June 2019;
Published online: 12 August 2019

References

1. Menviel, L., Timmermann, A., Timm, O. E. & Mouchet, A. Climate and biogeochemical response to a rapid melting of the West Antarctic Ice Sheet during interglacials and implications for future climate. *Paleoceanography* **25**, PA4231 (2010).
2. Bronselaer, B. et al. Change in future climate due to Antarctic meltwater. *Nature* **564**, 53–58 (2018).
3. DeConto, R. M. & Pollard, D. Contribution of Antarctica to past and future sea-level rise. *Nature* **531**, 591–597 (2016).
4. Golledge, N. R. et al. The multi-millennial Antarctic commitment to future sea-level rise. *Nature* **526**, 421–425 (2015).
5. Edwards, L. et al. Revisiting Antarctic ice loss due to marine ice-cliff instability. *Nature* **566**, 58–64 (2019).
6. Golledge, N. et al. Global environmental consequences of twenty-first-century ice-sheet melt. *Nature* **566**, 65–72 (2019).
7. Swingedouw, D. et al. Antarctic ice-sheet melting provides negative feedbacks on future climate warming. *Geophys. Res. Lett.* **35**, L17705 (2008).
8. Vizcaino, M., Mikolajewicz, U., Jungclaus, J. & Schurgers, G. Climate modification by future ice sheet changes and consequences for ice sheet mass balance. *Clim. Dynam.* **34**, 301–324 (2010).
9. Ma, H. & Wu, L. Global teleconnections in response to freshening over the Antarctic Ocean. *J. Clim.* **24**, 1071–1088 (2011).
10. Bintanja, R., Van Oldenborgh, G., Drijfhout, S., Wouters, B. & Katsman, C. Important role for ocean warming and increased ice-shelf melt in Antarctic sea-ice expansion. *Nat. Geosci.* **6**, 376–379 (2013).

11. Green, J. A. M. & Schmittner, A. Climatic consequences of a pine glacial collapse. *J. Clim.* **28**, 9221–9234 (2015).
12. Fogwill, C., Phipps, S., Turney, C. & Golledge, N. Sensitivity of the Southern Ocean to enhanced regional Antarctic ice sheet meltwater input. *Earth's Future* **3**, 317–329 (2015).
13. Golledge, N. R. et al. Antarctic contribution to meltwater pulse 1A from reduced Southern Ocean overturning. *Nat. Commun.* **5**, 5107 (2014).
14. Bakker, P., Clark, P. U., Golledge, N. R., Schmittner, A. & Weber, M. E. Centennial-scale Holocene climate variations amplified by Antarctic Ice Sheet discharge. *Nature* **541**, 72–76 (2017).
15. Sweet, W., Horton, R., Kopp, R., LeGrande, A. & Romanou, A. in *Climate Science Special Report: Fourth National Climate Assessment* Vol. I (eds Wuebbles, D. J. et al.) 333–363 (US Global Change Research Program, 2017).
16. Pollard, D., DeConto, R. M. & Alley, R. B. Potential Antarctic ice sheet retreat driven by hydrofracturing and ice cliff failure. *Earth Planet. Sci. Lett.* **412**, 112–121 (2015).
17. Jongma, J. I., Driesschaert, E., Fichefet, T., Goosse, H. & Renssen, H. The effect of dynamic– thermodynamic icebergs on the Southern Ocean climate in a three-dimensional model. *Ocean Model.* **26**, 104–113 (2009).
18. Stern, A., Adcroft, A. & Sergienko, O. The effects of Antarctic iceberg calving-size distribution in a global climate model. *J. Geophys. Res. Oceans* **121**, 5773–5788 (2016).
19. Rackow, T. et al. A simulation of small to giant Antarctic iceberg evolution: differential impact on climatology estimates. *J. Geophys. Res. Oceans* **122**, 3170–3190 (2017).
20. Tournadre, J., Bouhier, N., Girard-Ardhuin, F. & Remy, F. Antarctic icebergs distributions 1992–2014. *J. Geophys. Res. Oceans* **121**, 327–349 (2016).
21. Merino, N. et al. Impact of increasing Antarctic glacial freshwater release on regional sea-ice cover in the Southern Ocean. *J. Clim.* **20**, 436–448 (2007).
22. Stouffer, R. J., Seidov, D. & Haupt, B. J. Climate response to sources of freshwater: North Atlantic versus the Southern Ocean. *J. Clim.* **20**, 436–448 (2007).
23. Weaver, A. J., Saenko, O. A., Clark, P. U. & Mirtovica, J. X. Meltwater pulse 1A from Antarctica as a trigger of the Bølling-Allerød warm interval. *Science* **299**, 1709–1713 (2003).
24. McCreary, J. P., Furue, R., Schloesser, F., Burkhardt, T. W. & Nonaka, M. Dynamics of the Atlantic meridional overturning circulation and Southern Ocean in an ocean model of intermediate complexity. *Prog. Oceanogr.* **143**, 46–81 (2016).
25. Stocker, T. F. The seesaw effect. *Science* **282**, 61–62 (1998).
26. Bozbiyik, A., Steinacher, M., Joos, F., Stocker, T. & Menviel, L. Fingerprints of changes in the terrestrial carbon cycle in response to large reorganizations in ocean circulation. *Clim. Past* **7**, 319–338 (2011).
27. Menviel, L., Timmermann, A., Elison Timm, O. & Mouchet, L. Deconstructing the last glacial termination: the role of millennial and orbital-scale forcings. *Quat. Sci. Rev.* **30**, 1155–1172 (2011).
28. Trenberth, K. E., Fasullo, J. T. & Balmaseda, M. A. Earth's energy imbalance. *J. Clim.* **27**, 3129–3144 (2014).
29. Jourdain, N. et al. Ocean circulation and sea-ice thinning induced by melting ice shelves in the Amundsen Sea. *J. Geophys. Res. Oceans* **122**, 2550–2573 (2017).
30. Kidston, J., Taschetto, A. S., Thompson, D. W. J. & England, M. H. The influence of Southern Hemisphere sea-ice extent on the latitude of the mid-latitude jet stream. *Geophys. Res. Lett.* **38**, L15804 (2011).
31. Hillenbrand, C.-D. et al. West Antarctic Ice Sheet retreat driven by Holocene warm water incursions. *Nature* **547**, 43–48 (2017).
32. Stewart, A. L. & Thompson, A. F. Eddy-mediated transport of warm circumpolar deep water across the Antarctic shelf break. *Geophys. Res. Lett.* **42**, 432–440 (2015).

Acknowledgements

This research was supported by the National Science Foundation under award No. 1341394. A.T. is supported by the Institute for Basic Science, South Korea (Grant No. IBS-R028-D1).

Author contributions

F.S., A.T. and T.F designed the study. F.S conducted the model simulations and performed the analysis. F.S. and A.T. wrote the manuscript. T.F, R.D. and D.P. contributed to the writing of the manuscript. All authors contributed to interpreting the results and made substantial improvements to the manuscript.

Competing interests

The authors declare no competing interests.

Additional information

Supplementary information is available for this paper at https://doi.org/10.1038/s41558-019-0546-1.

Reprints and permissions information is available at www.nature.com/reprints.

Correspondence and requests for materials should be addressed to A.T.

Peer review information: *Nature Climate Change* thanks Nicolas Jourdain and the other, anonymous, reviewer(s) for their contribution to the peer review of this work.

Publisher's note: Springer Nature remains neutral with regard to jurisdictional claims in published maps and institutional affiliations.

Methods

LOVECLIM. The model used in this study is the coupled model of intermediate complexity LOVECLIM (LOch-Vecode-Ecbilt-CLio-agIsm Model), v.1.3. The atmospheric component of LOVECLIM is ECBilt[33], a spectral T21, three-level model based on quasi-geostrophic equations extended by estimates of the neglected ageostrophic terms[34]. The ocean component of LOVECLIM, CLIO[35–37], consists of a free-surface primitive equation model coupled to a thermodynamic-dynamic sea-ice model. The horizontal resolution is 3°×3° and the model has 20 vertical levels with 10-m thickness at the surface, which increases with depth. Coupling between atmosphere and ocean occurs via the exchange of freshwater, momentum and heat fluxes. A thermodynamic-dynamic iceberg model[17] is included in our model version, which allows for a more realistic thermodynamic and freshwater coupling of ocean and ice sheets. The iceberg model integrates iceberg trajectories subject to Coriolis force, air, water and sea-ice drag, horizontal pressure gradient force and wave radiation[17,38]. Iceberg melt takes into account basal and lateral melt and wave erosion along individual iceberg pathways[17,38]. LOVECLIM was implemented, and all experiments were performed, on Yellowstone at the NCAR-Wyoming Supercomputing Center and the University of Southern California High Performance Computing Center. The model was equilibrated with a 3,000-year run with constant, pre-industrial boundary conditions (the mean of the last 100 years of that run is used as pre-industrial control).

GHG emission scenarios. To explore the effect of freshwater forcing under different climatic conditions, we obtained LOVECLIM solutions under pre-industrial GHG concentrations and RCP8.5 and RCP4.5[39] GHG scenarios, respectively (Supplementary Fig. 1). Our LOVECLIM version has a climate sensitivity[40] comparable to that of CMIP5 models. In the control experiments with RCP8.5/RCP4.5 GHG concentrations and without MWF (RCP8.5–CTR/RCP4.5–CTR), SAT increased by about 4/2 K from 1950 to 2100 (Fig. 2), which is below the CMIP5 ensemble mean but well within the range of the CMIP5 model response.

Freshwater and icebergs. *Forcing scenarios.* The model is forced by simulated MWFs for scenarios RCP8.5 and RCP4.5 (AIS8.5 and AIS4.5 correspond to ensemble member Nos. 12 and AIS8.5b No. 5, respectively, in ref. [3]). Specifically, the amplitudes of these fluxes correspond to the simulated loss in Antarctic ice volume. In addition, we used synthetic AIS discharge scenarios with similar characteristics (Fig. 1) to test the climate impact of AIS forcing over a wide range of forcing strength.

The synthetic forcing scenarios are described by

$$\mathrm{MWF} = A\left(1+\tanh\frac{t-t_o}{\delta}\right)\frac{1+\exp\left[-\frac{(t-t_o)^2}{\delta^2}\right]}{\max(t_o,t)-2000} \quad (1)$$

where t is the forcing year, $t_o = 2120$ and timescale $\delta = 70, 73.3, \ldots, 90$ for scenarios S_i with $i = 1,\ldots, 7$, and the amplitude A is chosen such that the maximum amplitude is 1, 0.8, 0.6, 0.4, 0.2, 0.1, 0.05 Sv (1 Sv = 10^6 m^3 s^{-1}). For the forcing scenarios F_i, $i = 1,\ldots, 4$, the corresponding values are $t_o = 2150, 2160, 2170, 2180$, $\delta = 100$, 110, 120, 130 and the maximum amplitudes are 0.4, 0.3, 0.2 and 0.1 Sv. Control experiments without MWF were performed. The effect of the MWF is defined as the difference between forced and control experiments. To reduce the impact of internal variability on that difference, an ensemble of three experiments was obtained for each control experiment.

Enhanced ice-shelf calving due to hydrofracturing is the dominant mechanism by which ice is lost during major retreat of floating ice shelves[16]. Hence, the entire MWF is directed into the iceberg model in our standard set-up. In addition to the external MWF, there is an internal runoff into the Southern Ocean that balances net precipitation over the Antarctic continent (which was about 0.06 Sv for pre-industrial conditions and is increasing with rising temperatures, see Fig. 1a). This runoff is uniformly distributed over ocean grid boxes adjacent to the Antarctic coast. We tested the impact of including the entire MWF in the iceberg model by performing experiments where only half the flux goes into the iceberg model and the other half is distributed uniformly between 70 °S and the Antarctic coast (experiment 50/50), and where the entire flux is distributed south of 70 °S (experiment F70S). Note that LOVECLIM cannot simulate the circulation and melting in ice cavities, which may also impact the effect of meltwater[29].

Iceberg model. In the iceberg model, MWF is integrated in time and uniformly distributed on icebergs of three size classes (100 m × 100 m, 400 m × 400 m and 1 km × 800 m (width × height)). We tested additional size classes (200 m × 200 m, 300 m × 300 m and 700 m × 500 m; experiment CLASSES), which did not substantially alter iceberg impact. Accumulated icebergs are released every 5 d in equal proportion in the Weddell Sea (70 °S, 45 °W) and the Ross Sea (70 °S, 180 °E). We tested the release of icebergs from additional locations in the Admundsen Sea and off the Amery ice shelf (experiment LOCATION) as well as changing the partition between iceberg flux (experiments ROSS and WEDDELL), which modified the response regionally (Supplementary Fig. 6) but did not substantially change the large-scale impact of icebergs (Fig. 5). Note that the actual future iceberg size distribution is unknown and is not resolved by the ice-sheet/ice-shelf model[3]. Analysis of satellite images[41] indicates that most icebergs are advected by the Antarctic coastal current, before moving away from the Antarctic continent through iceberg alleys in the Weddell Sea and Ross Sea. Despite their relatively low numbers, ice volume is dominated by giant icebergs—longer than a few kilometres[20], which start melting significantly only in iceberg alleys as they progress into warmer water[19,42]. However, LOVECLIM does not resolve the narrow Antarctic coastal current well and current velocities are underestimated. Furthermore, giant icebergs provide a challenge for climate models as their dynamics differ from those of smaller icebergs[19]. For example, fragmentation plays an important role in the decay of giant icebergs[20], which cannot be simulated by current iceberg models. Due to their large volume, single iceberg trajectories could significantly impact melting patterns and hence require large ensembles[19].

Therefore, we do not include giant icebergs and smaller icebergs are released directly into iceberg alleys, to ensure that the pattern of iceberg melting is more realistic[18,19]. (Note that, in addition to this 'remote forcing', there is also meltwater input adjacent to the Antarctic coast due to internal runoff from Antarctica.) We specifically tested the different impacts of meltwater fluxes near and remote from the Antarctic coast by performing one experiment, F50SOFF, where the flux is uniformly distributed between 50 °S and Antarctica but at least two grid cells away from the Antarctic coast.

Melting icebergs require energy to account for latent heat. With specific latent heat $L = 334$ kJ kg^{-1} (ref. [43]) and density $\rho = 10^3$ kg m^3, sustaining a meltwater flux of 1 Sv requires an energy flux of

$$Q_{\mathrm{LH}} = \rho L \times 1\ \mathrm{Sv} = 0.33\ \mathrm{PW} \quad (2)$$

In our experiments, we neglect the energy required for warming the ice to melting point, which is generally small compared to the latent heat (the specific heat capacity of ice is ~2 kJ kg^{-1} K^{-1} near freezing point[44]). Freshwater and heat fluxes are both applied to the ocean surface layer along iceberg pathways. To illustrate the impact of cooling, we obtained additional model solutions where no heat is removed from the ocean for iceberg melting (including experiment No LH and F70S–no LH; see Supplementary Table 1).

Since iceberg pathways and melt are functions of various climate model variables, the freshwater and heat fluxes to the ocean component vary in space and time (see Supplementary Figs. 2 and 4). For example, forcing is stronger in summer than in winter because of enhanced iceberg melting[19], and trajectories are affected by changes in sea ice, winds and ocean circulation. The impact of such spatiotemporal variability is explored in sensitivity experiments where uniform meltwater and latent heat fluxes are directly applied to the ocean surface area between the Antarctic coast and 50 °S (F50S) and 70 °S (F70S), respectively. We also performed the experiment SEASON, which is identical to F70S except that fluxes have a seasonal cycle with an amplitude of 50% of the annual mean and reaches its maximum in February (see Supplementary Table 1). It is noteworthy that LOVECLIM reproduces the general temperature structure in the Southern Ocean with a subsurface temperature maximum; however, temperatures are biased toward cold by about one degree (Supplementary Fig. 5). Temperature biases of similar magnitude occur in most CMIP5 models in this region, and provided an additional challenge for simulation of realistic iceberg trajectories.

Data availability

The data that support the findings of this study are available from the corresponding author on request.

Code availability

The numerical model codes that support the findings of this study are available from the corresponding author on request.

References

33. Opsteegh, J., Haarsma, R., Selten, F. & Kattenberg, A. ECBILT: a dynamic alternative to mixed boundary conditions in ocean models. *Tellus A* **50**, 348–367 (1998).
34. Lim, G. H., Holton, J. R. & Wallace, J. M. The structure of the ageostrophic wind field in baroclinic waves. *J. Atmos. Sci.* **48**, 1733–1745 (1991).
35. Goosse, H., Deleersnijder, E., Fichefet, T. & England, M. Sensitivity of a global coupled ocean-sea ice model to the parameterization of vertical mixing. *J. Geophys. Res. Oceans* **104**, 13681–13695 (1999).
36. Goosse, H. & Fichefet, T. Importance of ice–ocean interactions for the global ocean circulation: a model study. *J. Geophys. Res. Oceans* **104**, 23337–23355 (1999).
37. Campin, J.-M. & Goosse, H. Parameterization of density-driven downsloping flow for a coarse-resolution ocean model in z-coordinates. *Tellus A* **51**, 412–430 (1999).
38. Bigg, G. R., Wadley, M. R., Stevens, D. P. & Johnson, J. A. Modelling the dynamics and thermodynamics of icebergs. *Cold Reg. Sci. Technol.* **26**, 113–135 (1997).

39. Meinshausen, M. et al. The RCP greenhouse gas concentrations and their extensions from 1765 to 2300. *Climatic Change* **109**, 213–241 (2011).
40. Timmermann, A. & Friedrich, T. Late Pleistocene climate drivers of early human migration. *Nature* **538**, 92–95 (2016).
41. Stuart, K. M. & Long, D. G. Iceberg size and orientation estimation using seawinds. *Cold Reg. Sci. Technol.* **69**, 39–51 (2011).
42. Merino, N. et al. Antarctic icebergs melt over the Southern Ocean: climatology and impact on sea ice. *Ocean Model.* **104**, 99–110 (2016).
43. Dickinson, H. C. & Osborne, N. S. Specific heat and heat of fusion of ice. *J. Wash. Acad. Sci.* **5**, 338–340 (1915).
44. Giauque, W. & Stout, J. The entropy of water and the third law of thermodynamics. The heat capacity of ice from 15 to 273 K. *J. Am. Chem. Soc.* **58**, 1144–1150 (1936).